ISSN No: 2348-4845
International Journal & Magazine of Engineering, Technology, Management and Research
A Peer Reviewed Open Access International Journal

Modular Multilevel Converter for Feeding Variable-Speed Drives of Cascaded Control System Using Fuzzy

S.Jayaprakash
M.Tech (PE)
Annamacharya Institute of Technology &Sciences, Tirupathi,Affiliated to JNTUA, Anatapur.

Mr.P.Muni Sekhar
Assistant Professor
Annamacharya Institute of Technology &Sciences, Tirupathi,Affiliated to JNTUA, Anatapur.

ABSTRACT

The design process of a holistic control system for a MMC to feed variable-speed drives is proposed in this paper.The performance of the control system is finally validated by measurements on a low-voltage MMC prototype, which feeds a field-oriented controlled induction machineFor high-power drive applications the modular multilevel converter (MMC) is an upcoming topology especially in the medium voltage range. First,from the analysis of the equivalent circuits the design of the current control for the independent adjustment of several current components is derived. Second, the current and voltage components by the investigation of the transformed arm power components for balancing the energies in the arms of the MMC are identified systematically. At minimum necessary internal currents over the complete frequency range The control system ensures a dynamic balancing of the energies in the cells of the MMC. Simultaneously, all other circulating current components are avoided to minimize current stress and additional voltage pulsations.. Here we are using the fuzzy controller compared to other controllers i.e. The fuzzy controller is the most suitable for the human decision-making mechanism, providing the operation of an electronic system with decisions of experts. In addition, using the fuzzy controller for a nonlinear system allows for a reduction of uncertain effects in the system controland improve the efficiency.A cascaded structure with subordinated current control loops and filter-based energy control loops is proposed in this paper.Simulation results are shown below.

Key Terms – Modular multilevel converters (MMC), Variable–speed drives, control theory, fuzzy controller.

1. INTRODUCTION

Now a day's many industrial applications have begun to require high power Some medium voltage motor drives and utility applications require medium voltage. The multi level inverter has been introduced since 1975 as alternative in high power and medium voltage situations. The Multi level inverter is like an inverter and it is used for industrial applications as alternative in high power and medium voltage situations. **T**he modular multilevel converter (MMC) was introduced in 2002 [1] as dc–3ac configuration .For high-voltage dc power transmission the use of this topology for feeding electrical drives in the range of medium voltage was proposed in [2]and [3]. First, experimental results with low-voltage prototypes of MMC-based drive converters are shown in [4] and [5]. At low frequencies or even standstill the increasing amount of the energy pulsation in the capacitors of the cells is reduced to acceptable values by the use of an ac common mode voltage with corresponding inner currents. which is necessary for variable-speed drives at low frequency was solved in [6]. This is most challenging issue of operating the MMC. An appropriate

ISSN No: 2348-4845
International Journal & Magazine of Engineering, Technology, Management and Research
A Peer Reviewed Open Access International Journal

control scheme, especially for this low-frequency mode, is presented in [7] and [8].

Here, a cascaded structure with subordinated current control loops and filter-based energy control loops is proposed. . The performance of the control system is finally validated by measurements on a low-voltage MMC prototype, which feeds a field-oriented controlled induction machineDue to a possible harmonic content however, in [12]–[14], no waveform of the dc current is shown, which is also an important aspect regarding additional current stress of the dc-voltage source

MODELING OF PROPOSED THEORY

I. A. Structure, Fundamentals, and Definitions of the MMC

In Fig. 1 the complete system including the dc-voltage source, the MMC itself, and the three-phase machine is illustrated [11]. The MMC includes three phases, each with an upper armpand a lower arm n. The currents in the arms are defined as ixy(upper or lower arm: x ∈ {p,n }, no. of phase: y ∈ {1, 2, 3 }). One converter arm is built by m cells (no. of cell:

By switching the half bridges of the cells, each arm is able to generate an adjustable arm voltage uxywith m+1 voltage steps.

Due to the half bridges in the cells and a pulsewidth modulation (PWM) of at least one cell, the range of the specific arm voltage is

$$0 \le u_{xy} = \sum_{z=1}^{m} u_{xyz} \le u_{c_{xy}} = \sum_{z=1}^{m} u_{c_{xyz}} \qquad (1)$$

BLOCK DIGRAM

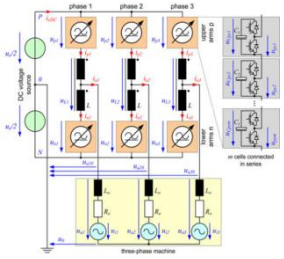

Fig. 1.Schematic of the MMC with the definitions of voltages and currents.

Here, uCxyis the sum of the capacitors' voltages of all cells in the arm xy. These voltages uCxycorrespond to the arm energies wxy. The time-variant arm energies w˜xy(t) are determined by the integration of the arm power pxyassuming that the balancing task will ensure constant arm energies w¯C

$$\hat{w}_{xy}(t) = \int_0^t u_{xy}(T).\, i_{xy}(T)\partial T = P_{xy}\,(T) \qquad (2)$$

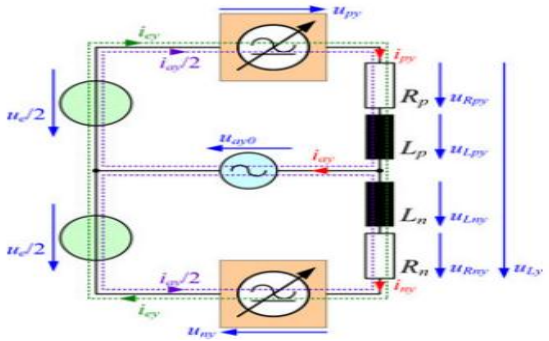

Fig. 2. Equivalent circuit of one phase of the MMC

Hence, the components of the capacitor voltages and the corresponding arm energies become equal

$$u_{Cxy}^2(t) = \left(\bar{u}_C + \bar{u}_{Cxy}(t)\right)^2 = \frac{2m}{C_s}.\left(\bar{w}_C + wxyt\right)(3)$$

The MMC generates the phase voltages uay0 related to the midpoint 0 of the dc source on the three-phase ac side. The common-mode voltage u0 of the neutral point of the threephase machine is also related to the reference potential of the dc-voltage source. By the Clarke-transformation of (43)the phase voltages uay0 as well as the phase currents iayare transformed to the αβ0-components of the corresponding space vectors

$$\begin{bmatrix} u_{a\alpha} \\ u_{a\beta} \\ u_0 \end{bmatrix} = C.\begin{bmatrix} u_{a10} \\ u_{a20} \\ u_{a30} \end{bmatrix}\begin{bmatrix} i_{a\alpha} \\ i_{a\beta} \\ 1_{a0} \end{bmatrix} = C.\begin{bmatrix} i_{a1} \\ i_{a2} \\ i_{a3} \end{bmatrix} (4)$$

By their polar coordinates these Cartesian components could also be expressed

$$u_{a\alpha} = \hat{u}_a.\cos(\gamma_a)\, i_{a\alpha} = \hat{\imath}_a.\cos(\gamma_a - \varphi_a) \quad (5)$$

$$u_{a\beta} = \hat{u}_a.\sin(\gamma_a)\, i_{a\beta} = \hat{\imath}_a.\sin(\gamma_a - \varphi_a)\ (6)$$

ISSN No: 2348-4845
International Journal & Magazine of Engineering, Technology, Management and Research
A Peer Reviewed Open Access International Journal

II. DECOUPLED CURRENT CONTROL OF THE MMC

A. Analysis and Transformation of the MMC Network

Each arm current *I xy*consists of the components belonging to the dc side *Iey*and half of the phase current *iay*(see Fig. 2)

$$i_{py} = i_{ey} + \frac{i_{ay}}{2} i_{ny} = i_{ey} - \frac{i_{ay}}{2} \qquad (7)$$

The differential equations of *iey*and *iay*follow from the analysis of the equivalent circuit of one phase of the MMC in Fig. 2, see [7], [8], and [15]

$$i_{ey} = \frac{1}{2L}.\left(u_e - u_{py} - u_{ny} - 2R.\, i_{ey}\right) \qquad (8)$$

$$i_{ay} = \frac{1}{L}.\left(-2u_{ay} - u_{py} + u_{ny} - R.\, i_{ay}\right) \quad (9)$$

The impedances of the *p*- and *n*-arms are assumed to be equal (*R* = *Rp*= *Rn*,*L* = *Lp*= *Ln*).

$$\begin{bmatrix} u_{x\alpha} \\ u_{x\beta} \\ u_{x0} \end{bmatrix} = C.\begin{bmatrix} u_{x1} \\ u_{x2} \\ u_{x3} \end{bmatrix}\begin{bmatrix} I_{e\alpha} \\ u_{e\beta} \\ u_{e0} \end{bmatrix} = C.\begin{bmatrix} i_{e1} \\ i_{e2} \\ i_{e3} \end{bmatrix}. \qquad (10)$$

Replacing the arm voltages and the e-currents in (8) by these *αβ*0-components yields to the following differential equations, which are illustrated as equivalent circuits in Fig. 3:

$$\begin{bmatrix} I_{e\alpha} \\ u_{e\beta} \\ u_{e0} \end{bmatrix} = C.\begin{bmatrix} i_{e1} \\ i_{e2} \\ i_{e3} \end{bmatrix} = \frac{1}{2L}\begin{bmatrix} -u_{p\alpha} - u_{n\alpha} - 2R.\, i_{e\alpha} \\ -u_{p\beta} - u_{n\beta} - 2R.\, i_{e\beta} \\ u_e - u_{p0} - u_{n0} - 2R.\, i_{e0} \end{bmatrix} \quad (11)$$

The same procedure is performed with the currents at the 3ac side of (9) by the use of the transformation of the phase values

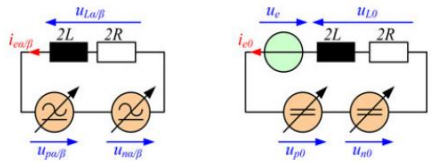

Fig. 3.Resulting equivalent circuits of the transformed e-current components.

According to (4)

$$\begin{bmatrix} u_{a\alpha} \\ u_{a\beta} \\ u_0 \end{bmatrix} = \frac{1}{2}\begin{bmatrix} -u_{p\alpha} - u_{n\alpha} - R.\, i_{a\alpha} - L.\, i_{a\alpha} \\ -u_{p\beta} + u_{n\beta} - R.\, i_{a\beta} - L.\, i_{a\beta} \\ -u_{p0} + u_{n0} \end{bmatrix} \qquad (12)$$

In the phases of the MMC the voltages $-L \cdot \dot{i}\, a\alpha/\beta$ will be zero if magnetically coupled inductors are used (see Fig. 1). The voltage drops of the resistance $-R \cdot ia\alpha/\beta$ are neglected. They will be compensated by the current controllers of *iaα/β* .

B. Voltage Components for the Current Control

The three control voltages *uLα/β/*0 of the corresponding e-currents The voltages across the impedances are summarized to, see Fig. 3

$$u_{L\alpha/\beta/0} = 2L.\, i_{e\alpha/\beta/0} + 2R.\, i_{e\alpha/\beta/0} \qquad (13)$$

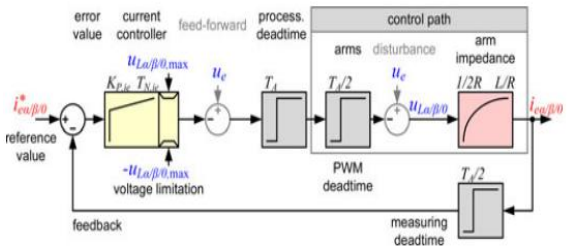

Fig. 4. Current control loops of the e-currents in transformed components

This current corresponds to the zero sequence component *ie*0 , which is the mean value of all six-arm currents, by *ie*DC = 3*ie*0 . These control voltages allow a specific and independent adjustment of the internal currents *ieα* and *ieβ* (often denoted as circulating currents) as well as the current of the dc-side *ie*DC .By solving the system of equations of (11) and (12) the composition of the six-arm voltages *uxy*is achieved. The inverse transformation of the *αβ*0-components of the *p*- and *n*-arms yields to the reference values of the arm voltages

$$\begin{bmatrix} u^*_{p1} \\ u^*_{p2} \\ u^*_{p3} \end{bmatrix} = C^{-1}.\begin{bmatrix} -\frac{1}{2}u_{L\alpha} - u_{a\alpha} \\ -\frac{1}{2}u_{L\beta} - u_{a\beta} \\ \frac{1}{2}u_e - \frac{1}{2}u_{L0} - u_0 \end{bmatrix} \qquad (14)$$

ISSN No: 2348-4845
International Journal & Magazine of Engineering, Technology, Management and Research
A Peer Reviewed Open Access International Journal

$$\begin{bmatrix} u^*_{n1} \\ u^*_{n2} \\ u^*_{n3} \end{bmatrix} = C^{-1}.\begin{bmatrix} -\frac{1}{2}u_{L\alpha} + u_{a\alpha} \\ -\frac{1}{2}u_{L\beta} + u_{a\beta} \\ \frac{1}{2}u_e - \frac{1}{2}u_{L0} + u_0 \end{bmatrix} \quad (15)$$

The energy balancing of the cells inside of each arm [7], [10], [16], see Figs. 5 and 7. By the modulator, these six reference values have to be converted to the corresponding switching states for the cells which has to include This approach enables, in addition to the decoupled control of the internal currents *I eα/β* and the dc current *ie*0 / *ie*DC ,by the corresponding voltage system *uaα/β* , see (12), the independent and individual adjustment of the three-phase current system *iaα/β*

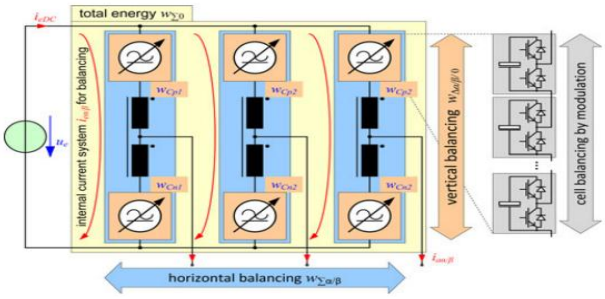

Fig. 5.Energy control and balancing tasks in the MMC.

The common-mode voltage *u*0 can be freely adjusted within the limits of the arm voltages *uxy*, which depend on the instantaneous sum of the capacitor voltages *uCxy*, see (1). It consists of two components

$$u_0 = -\frac{1}{6}\hat{u}_a.\cos(3\gamma_a) + \hat{u}_0.\cos(\omega_0 . t) \quad (16)$$

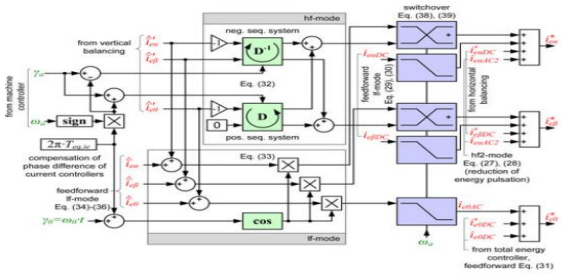

Fig. 6. Estimation of the e-current reference values

At low-frequency operation [6], [7],The part *u*0*e* is used as degree of freedom for the balancing task which is described later. For increasing the output voltage the part *u*0*a* is used by factor 2/√3 with the third harmonic of *γa*for the over modulation.. Here, an ac component with the amplitude *u*ˆ 0 and an arbitrary frequency *ω*0 is set

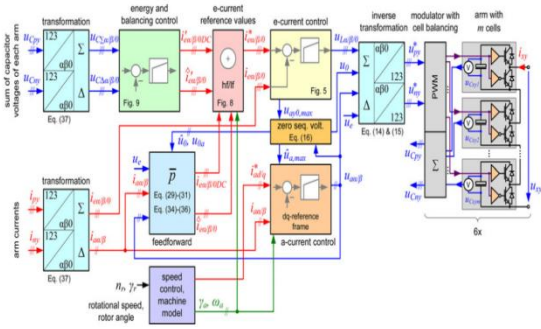

Fig. 7. Signal flow path of complete MMC control system with subordinate current controllers, arm energy balancing, motor control unit, and modulator.

C. Function of the Arm Inductance

In this approach, the inductances allow the individual adjustment of the several currents by the respective current control loops with the voltage components. The inductances *L* decouple the six voltage sources realized by the arms of the MMC of To use the inductance for damping the internal currents in the range of the output frequency it is proposed. On the basis of the switching states of the cells and accordingly with the modulation schemethe inductance *L* has to be dimensioned.

It depends on the switching frequency *f*PWM of the PWM, if one cell per arm and switching cycle is modulated, and on the cell voltage *uC xyz*. To sum up, the inductance *L* is determined by the maximum allowed ripple content of the dc and inner currents Δ*iey*. Consequently, the value of the inductance *L* is determined by the voltages on the level of the cells and not by the voltages or currents of the arms. This yields to a relative small value of the inductance *L*.

D. Current Control Loops of the MMC

As shown in Fig 3,by the corresponding voltages *uLα* ,*uLβ* , and*uL*0 each control loop incorporates the impedances (*L*, *R*) of the arms, in which the current components have to be controlled, The three current control loops, see Fig. 4, for *ieα* , *ieβ* , and *ie*0 are derived by the equivalent circuits of Fig. 3 and their equations (11). The measured value of the dc voltage

ISSN No: 2348-4845
International Journal & Magazine of Engineering, Technology, Management and Research
A Peer Reviewed Open Access International Journal

*ue*is used as feed forward in the control loop of*ie*0 , see Fig. 4. by a time-discrete P- or PI-controller (P: proportional, I: integral) with the sampling time *TA* each current controller is realized. The dead times of the measurement, signal processing, and PWM are included by the sum of the small time constants *T σ,ie*=2*TA* . Then, the maximum gain of the proportional part of the controller is [18]

$$K_{P,ie} = \frac{T_{S,ie}}{2V_{s,ie}.T_{\sigma.ie}} = \frac{\frac{L}{R}}{\frac{2}{2R}.2T_A} = \frac{L}{2T_A} \quad (17)$$

A P-controller will be sufficient Due to the fact, that the energy controllers will be superposed,.especially for the dc-current *ie*0 for compensating the time constantThe I-part of the current controller could be used *T N,ie*= *TS,ie*= *L/R*.*VS,ie*=1/2*R* is the gain of the control path and *TS,ie*= *L/R* the corresponding time constant Consequently, the dynamic behavior of the closed control loops corresponds approximately to a first-order time-delay element with the equivalent time constant *T* eq,ie =2*Tσ,ie* =4*TA* .

III. BALANCING OF THE ARM ENERGIES

A. Transformation of Arm Power Components

For the balancing of the six-arm energies *wxy*, First, the upper and lower power components are converted to their mean value and difference

$$p\sum y = \frac{1}{2}(p_{py} + p_{ny}) = \frac{1}{2}(u_{py}i_{py} + u_{ny}i_{ny}) \quad (18)$$

$$p\Delta_y = p_{py} - p_{ny} = u_{py}i_{py} - u_{ny}i_{ny} \quad (19)$$

Second, these power components are transformed by the Clarke matrix **C** to the *αβ*0-components

B. Energetic Analysis of the Arm Energies in Transformed Values for the Identification of the Balancing Currents

In steady-state operation the mean value of each power component $p\bar{\Sigma}/\Delta\alpha/\beta/0$ has to be zero for a symmetrical energy distribution,depending on the frequency *ωa*of the three-phase currents *Iay*. Here, two methods of energy balancing have to be distinguished . Ifis high enough, which yields to the rotation of the phase angle by *γa*= *ωa* ·*t* over the time *t*, even at standstill respectively at frequency *ωa*=0.

this allows the stable operation of the MMC

1) Horizontal Balancing:

For the balancing in horizontal direction, the energy transfer between the three phases of the MMC see Fig. 5, is achieved by the dc-components of the inner currents I eαDC and ieβDC. According to (21) and (22), they generate together with the dc voltage ueactive power components in pΣα and pΣβ see Table I. In each phase of the MMC occurs a dominant energy pulsation with the second harmonic of the output frequency ωa. By additional inner ac currents I eα,hf2 and ieβ,hf2 this power component could be compensated for reducing the energy pulsation in the arms (hf2-mode), see [19]

$$i_{e\alpha}AC_2 = \frac{1}{2u_e}.\hat{u}_a.\hat{i}_a.\cos(2\gamma_a - \varphi_a) \quad (20)$$

$$i_{e\beta}AC_2 = -\frac{1}{2u_e}.\hat{u}_a.\hat{i}_a.\sin(2\gamma_a - \varphi_a) \quad (21)$$

TABLE I
OVERVIEW OF THE POWER COMPONENTS FOR BALANCING THE ARM ENERGIES IN TRANSFORMED VALUES

	power	voltage	current	frequency	comment
horizontal	$\bar{p}_{\Sigma\alpha}$	$u_e/2$	$i_{e\alpha DC}$	DC	
	$\bar{p}_{\Sigma\beta}$	$u_e/2$	$i_{e\beta DC}$	DC	
mean/total	$\bar{p}_{\Sigma 0}$	$u_e/2$	i_{e0DC}	DC	
vertical (hf)	$\bar{p}_{\Delta\alpha,hf}$	$\hat{u}_a$	$-\hat{i}_{ed-}$	ω_a	neg. seq.
	$\bar{p}_{\Delta\beta,hf}$	$\hat{u}_a$	$+\hat{i}_{eq-}$	ω_a	
	$\bar{p}_{\Delta 0,hf}$	$\hat{u}_a$	$-\hat{i}_{ed+}$	ω_a	pos. seq.
vertical	$\bar{p}_{\Delta\alpha/\beta/0,lf}$	$\hat{u}_0$	$\hat{i}_{e\alpha/\beta/0}$	ω_0	zero seq.

The power components −*u*0 ·*iaα/β* and ±*uaα/β* ·*iaα/β* have to be compensated at low-output frequency or stationary space vectors (*ωa*=0), .This yields to the following internal dc-current components in the lf-mode:

$$i_{e\alpha}DC = \frac{1}{2u_e}(u_{a\alpha}.i_{a\alpha} - u_{a\beta}.i_{a\beta} + 2u_{0a}.i_{a\alpha}) \quad (22)$$

$$i_{e\beta}DC = \frac{1}{2u_e}(-u_{a\alpha}.i_{a\beta} - u_{a\beta}.i_{a\alpha} + 2u_{0a}.i_{a\beta}) \quad (23)$$

2)Mean Energy Control:

By the difference between the dc power and the 3ac active power *Pa* ,The total energy stored in all cells of the MMC is influenced shown in 23.The dc current for the power exchange with the dc-voltage source *ue*will be without losses

ISSN No: 2348-4845
International Journal & Magazine of Engineering, Technology, Management and Research
A Peer Reviewed Open Access International Journal

$$i_{eDC} = \frac{1}{2u_e}.\left(u_{\alpha\alpha}.i_{\alpha\alpha} + u_{\alpha\beta}.i_{\alpha\beta}\right) = \frac{1}{3}i_{eDC} \qquad (24)$$

3) Vertical Balancing:

Between the upper and lower arms of the MMCThe vertical balancing task ensures an energy equilibrium, see Fig. 5. between the upper and lower arms of the MMC these methods can be used in the hf-mode, x enough. The internal 3ac-current system is divided in its symmetrical components (positive and negative sequence components), [20], where **D** is the rotation matrix of (44) according to the phase angle *γa*

$$\begin{bmatrix} i_{caAC} \\ i_{e\beta AC} \end{bmatrix} = D(\gamma_0).\begin{bmatrix} \hat{\imath}_{ed+} \\ \hat{\imath}_{eq+} \end{bmatrix} + D^{-1}(\gamma_a).\begin{bmatrix} \hat{\imath}_{ed-} \\ \hat{\imath}_{eq-} \end{bmatrix} \qquad (25)$$

By their *dq*-components of the corresponding amplitudes the positive as well as the negative sequence components of the current system are expressed. By the common-mode voltage *u*0 and the e-currents *ieα/β/*0Corresponding active power components have to be independently generated . This is realized by the ac component *u*0*e* according to (16) together with the three ac current components *ieα/β/*0 at the same frequency and phase [6], [7], [21]

$$\mathrm{i}_{e\alpha/\beta/0\ AC} = \hat{\mathrm{i}}_{e\alpha/\beta/0}.\cos(\gamma_0) \quad (26)$$

At stationary space vectors for a balanced energy distribution in vertical direction the transformation of the pΔα/β power of (21) and (25) delivers the values of the amplitudes for the internal currents

$$\hat{\mathrm{I}}_{e\alpha} = \frac{1}{\hat{\mathrm{u}}_{0e}}\left(\frac{1}{2}\mathrm{u}_e\mathrm{i}_{a\alpha} - 2\mathrm{u}_{a\alpha}.\mathrm{i}_{e0DC} - 2\mathrm{u}_{0\alpha}\mathrm{i}_{e\alpha DC} - \mathrm{u}_{a\alpha}\mathrm{i}_{e\alpha DC} + \mathrm{u}_{\alpha\beta}.\right) \qquad (27)$$

$$\hat{\mathrm{I}}_{e\beta} = \frac{1}{\hat{\mathrm{u}}_{0e}}\left(\frac{1}{2}\mathrm{u}_e\mathrm{i}_{a\beta} - 2\mathrm{u}_{a\beta}\mathrm{i}_{e0DC} - 2\mathrm{u}_{0a}\mathrm{i}_{e\beta DC} + \mathrm{u}_{a\alpha}\mathrm{i}_{e\beta DC} + \mathrm{u}_{\alpha\beta}.\mathrm{i}_{e\alpha DC}\right) \qquad (28)$$

The *p*Δ0 power of (26) causes a superposed ac component in the current of the dc side *i eDC* respectively *i*

$$\hat{\mathrm{I}}_{e0} = \frac{1}{\hat{\mathrm{u}}_{0e}}\left(-2\mathrm{u}_{0DC}.\mathrm{i}_{e0DC} - \mathrm{u}_{a\alpha}.\mathrm{i}_{e\alpha DC} - \mathrm{u}_{\alpha\beta}\mathrm{i}_{e\beta DC}\right) \qquad (29)$$

This ac current occurs only in the lf-mode and is comparatively small, but has to be tolerated by the dc-voltage source *ue*

IV. CONTROL SYSTEM OF THE MMC FOR VARIABLE-SPEED DRIVES

According or the MMC drive system is illustrated in Fig. 7. The complete control system f *y* of each arm as well as the six-arm currents *I xy*are measured and transformed The six sums of the capacitor voltages *uC x* to Section III-A to their related components, see Table I (here: $x \in \{uC,i\}$)

$$\begin{bmatrix} x\varepsilon o \\ x\varepsilon o \\ x\varepsilon o \end{bmatrix} = \frac{1}{2}C.\begin{bmatrix} x_{p1} + x_{n1} \\ x_{p2} + x_{n2} \\ x_{p3} + x_{n3} \end{bmatrix}.\begin{bmatrix} x\Delta o \\ x\Delta o \\ x\Delta o \end{bmatrix} = C.\begin{bmatrix} x_{p1} - x_{n1} \\ x_{p2} - x_{n2} \\ x_{p3} - x_{n3} \end{bmatrix} \qquad (30)$$

From its superposed speed controller the five-current components are routed to their current controllers, The a-current controller of the three-phase machine receives its reference values in *d*- and *q*-components.To calculate the reference angle *γa*and the corresponding electrical frequency *ωa* the machine model in the speed controller has for the *dq*-current controller as well as for the phase angles of the internal ac balancing currents

A. Switchover of the Current References

According to the generation of the active power components for the balancing tasks (see Table I). the current references have to be switched over between the lf- and hf-mode.By a linear switchover between the effective current components this is realized

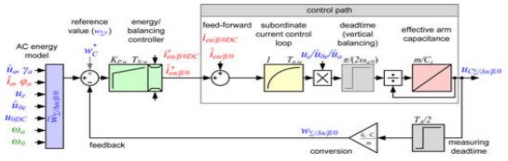

Fig. 8. Effective control loop for balancing the arm energies of the MMC.

ISSN No: 2348-4845
International Journal & Magazine of Engineering, Technology, Management and Research
A Peer Reviewed Open Access International Journal

These factors are calculateddepending on the weighting factors *klf*and *khf* by a linear relation to the electrical frequency *ωa*

$$k_{hf}(\omega_a) = \begin{cases} 0 & \text{if} |\omega_a| \le \omega_{a1} \\ \frac{|\omega_a| - \omega_{a1}}{\omega_{a2} - \omega_{a1}} & \text{if} |\omega_a| \le |\omega_a| < \omega_{a2} \\ 1 & \text{if} \omega_{a2} \le |\omega_a| \end{cases} \quad (31)$$

$$k_{hf}(\omega_a) = 1 - k_{hf}(\omega_a) \quad (32)$$

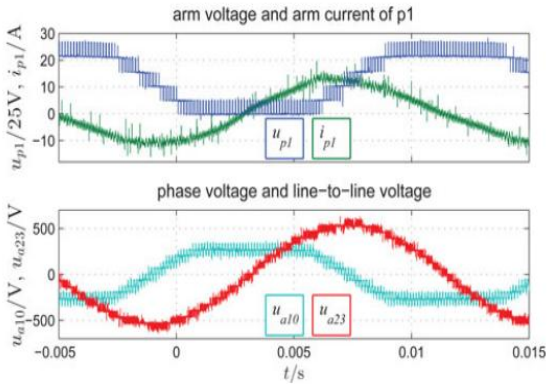

Fig. 9. Measured voltage and current waveforms of the MMC prototype

The mean value of the references of the other five balancing controllers has to be zero to achieve a symmetrical energy distribution in the arms.This reference value is twice the desired mean values $w^{-}C$of the arm energies. On the basis of the measured currents, reference voltages, frequencies, and phase angles, see Fig. 8.to avoid this issue, the pulsating parts of the energies are calculated by an ac energy.

$$w_c^* = \frac{\bar{u}_c^2 . C_z}{m} = 2\bar{w}_C \quad (33)$$

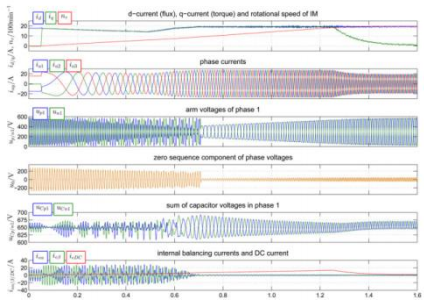

Fig. 10. Run-up of a field-oriented controlled induction machine fed by the MMC prototype, short time averaged values at TA =1/fPW M =1/(8 kHz).

The maximum gain *KP,wΣ* of the energy controller (*wΣ*0) and the horizontal balancing controllers (*wΣα/β*) is estimated compared to the design of the current controllers

$$K_{p,u} = \frac{1}{u_e.(\frac{T_A}{2} + T_{\sigma,ie})} \quad (34)$$

Due to the generation of the active power by the ac voltages and currents have to be included in the gain of the controllers in the vertical balancing control loops, the different voltages of *uˆ a* and *uˆ* 0 , as well as the dominant mean dead time

$$k_{p,w\Delta} = \frac{1}{\pi} . \left(k_{hf} . \frac{|\omega_a|}{\hat{u}_a} + k_{lf} . \frac{|\omega_0|}{\hat{u}_0} \right) \quad (35)$$

To improve the tracking performance at steady-state operation an additional integral part of the controller could be used. lf-mode is calculated on the basis of the residual part of the arm voltages *uxy*. Here, the voltages *uLα/β*/0 for the e-current control are subtracted in consideration of the necessary voltage amplitude *uˆ a* for the machine and the Overmodulation by *u*0*a* according to (16), which yields to the limits *u ay*0,max and *uˆ a*,max in Fig. 7.

V FUZZY LOGIC CONTROLLER

FLC is one of the most successful operations of fuzzy set theory. Its chief aspects are the exploitation of linguistic variables rather than numerical variables. FL control technique relies on human potential to figure out the system behavior and is constructed on quality control rules.. The basic structure of an FLC is represented in Fig.6.

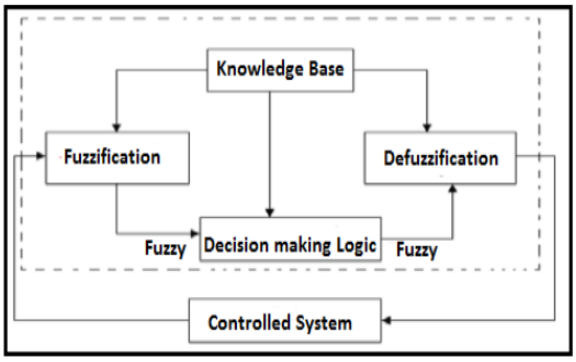

Fig.11 Basic structure of Fuzzy Logic controller

ISSN No: 2348-4845
International Journal & Magazine of Engineering, Technology, Management and Research
A Peer Reviewed Open Access International Journal

• A Fuzzification interface alters input data into suitable linguistic values.

• A Knowledge Base which comprises of a data base along with the essential linguistic definitions and control rule set.

• A Decision Making Logic which collects the fuzzy control action from the information of the control rules and the linguistic variable descriptions

• A Defuzzification interface which surrenders a non fuzzy control action from an inferred fuzzy control action. In this paper, an advanced control strategy, FLC is implemented along with UPQC for voltage correction through Series APF and for current regulation through Shunt APF. Error and Change in Error are the inputs and Duty cycle is the output to the Fuzzy Logic Controller as shown in Fig. 7-Fig.9

TABLE II.fuzzy rule representation

Change in error	Error						
	NB	NM	NS	Z	PS	PM	PB
NB	PB	PB	PB	PM	PM	PS	Z
NM	PB	PB	PM	PM	PS	Z	Z
NS	PB	PM	PS	PS	Z	NM	NB
Z	PB	PM	PS	Z	NS	NM	NB
PS	PM	PS	Z	NS	NM	NB	NB
PM	PS	Z	NS	NM	NM	NB	NB
PB	Z	NS	NM	NM	NB	NB	NB

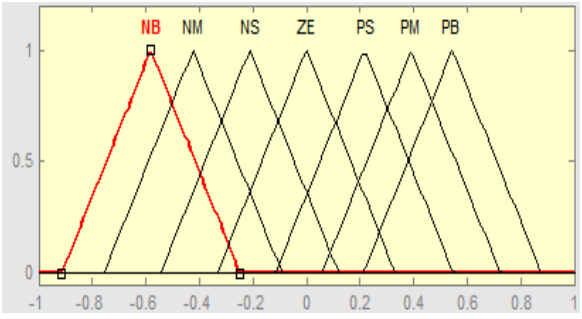

Fig 12.input error membership functins

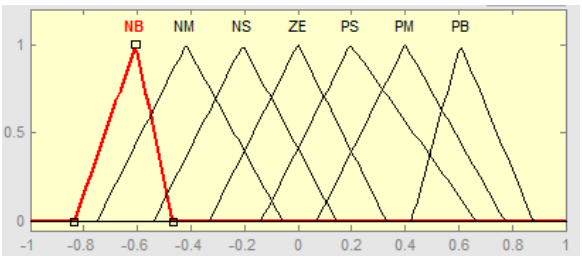

Fig 13.changing error as input membership functions

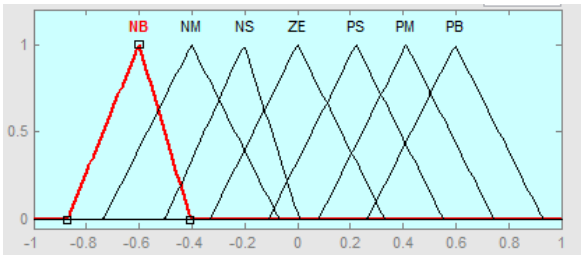

Fig 14.Output of the variable membership functions

In the decision-making process, there is rule base that links between input (error signal) and output signal. Table II shows the rule base exercised in this proposed Fuzzy Logic Controller.

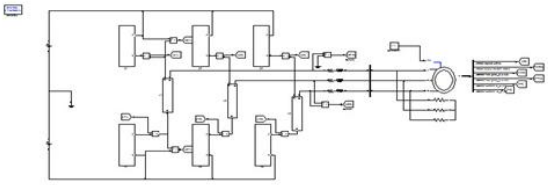

Fig 15. Block diagram of the simulation

VI. CONCLUSION

The control and balancing system of the MMC allows the supply of three-phase machines independent of their type and motor control system is proposed in this paper .On the base of the analysis of the equivalent circuit as well as of the active power components in the armsa cascaded control system for the MMC to feed variable speed drives is derived. At minimum internal currents the realization by the transformation of all relevant values allows a dynamic control of the arm energies over the complete operation range of the drive. For the balancing tasks the systematical design process of the several controllers and feed-forward components are presented.A cascaded structure with subordinated current control loops and filter-based energy control loops is proposed in this paper.Here we are using the fuzzy controller compared to other controllers i.e. The fuzzy controller is the most suitable for the human decision-making mechanism, providing the operation of an electronic system with decisions of experts. In addition, using the fuzzy controller for a nonlinear system allows for a reduction of uncertain effects in the system controland improve the efficiency. Finally,the performance of the control system the measurement at a

MMC prototype combined with a field-oriented control of an induction machine validates the approach and illustrated by using the simulation results.

REFERENCES

[1] Johannes Kolb, Felix Kammerer, Mario Gommeringer, and Michael Braun,"Cascaded ControlSysytem of the Modular Multilevel Converter for Feeding Variable-Speed Drives,"¨IEEETrans.Power Electron., vol.30,No.1, pp.349-357,January.2016.

[2] R.Marquardt,A.Lesnicar,andJ.Hildinger, "ModularesStromrichterkonzept fur NetzkupplungsanwendungenbeihohenSpannungen,"¨presented at the ETG-Fachtagungen, Bad Nauheim, Germany, 2002.

[3] M. Hiller, D. Krug, R. Sommer, and S. Rohner, "A new highly modular medium voltage converter topology for industrial drive applications," in Proc. 13th Eur. Conf. Power Electron. Appl., 2009, pp. 1–10.

[4] M. Hagiwara, K. Nishimura, and H. Akagi, "A modular multilevel PWM inverter for medium-voltage motor drives," in Proc. IEEE Energy Convers.Congr.Expo., 2009, pp. 2557–2564.

[5] M. Hagiwara, K. Nishimura, and H. Akagi, "A Medium-Voltage Motor Drive With a Modular Multilevel PWM Inverter," IEEE Trans. Power Electron., vol. 25, no. 7, pp. 1786–1799, Jul. 2010.

[6] A. Antonopoulos, K. Ilves, L. Angquist, and H.-P Nee, "On interaction between internal converter dynamics and current control of highperformance high-power AC motor drives with modular multilevel converters," in Proc. IEEE Energy Convers. Congr.Expo., 2010, pp. 4293– 4298.

[7] A. Korn, M. Winkelnkemper, and P. Steimer, "Low output frequency operation of the Modular Multilevel Converter," in Proc. IEEE Energy Convers. Congr.Expo., 2010, pp. 3993–3997

[8] J. Kolb, F. Kammerer, and M. Braun, "A novel control scheme for low frequency operation of the Modular Multilevel Converter," in Proc. Power Electron., Intell.Motion Energy Manag. Eur., 2011, pp. 977–982.

[9] J. Kolb, F. Kammerer, and M. Braun, "Straight forward vector control of the Modular Multilevel Converter for feeding three-phase machines over their complete frequency range," in Proc. 37th Annu. Conf. IEEE Ind. Electron. Soc., 2011, pp. 1596–1601.

[10] J. Kolb, F. Kammerer, P. Grabherr, M. Gommeringer, and M. Braun, "Boosting the efficiency of low voltage modular multilevel converters beyond 99%," in Proc. Power Electron., Intell. Motion Energy Manag. Eur., 2013, pp. 1157–1164.

[11] J. Kolb, F. Kammerer, and M. Braun, imensioning and design of a Modular Multilevel Converter for drive applications," in Proc. 15th Int. Power Electron. Motion Contr. Conf., 2012, pp. LS1a-1.1-1–LS1a-1.1-8.

[12] J. Kolb, F. Kammerer, and M. Braun, "Operating performance of modular multilevel converters in drive applications," in Proc. Power Electron., Intell.Motion Energy Manag. Eur., Nuremberg, Germany, 2012, pp. 583– 590.

[13] A. Antonopoulos, L. Angquist, S. Norrga, K. Ilves, and H.-P.Nee, "Modular multilevel converter ac motor drives with constant torque form zero to nominal speed," in Proc. IEEE Energy Convers.Congr.Expo., 2012, pp. 739–746.

[14] M. Hagiwara, I. Hasegawa, and H. Akagi, "Start-up and low-speed operation of an electric motor driven by a modular multilevel cascade inverter," IEEE Trans. Ind. Appl., vol. 49, no. 4, pp. 1556–1565, Jul./Aug. 2013.

[15] J.-J. Jung, H.-J.Lee, and S.-K. Sul, "Control strategy for improved dynamic performance of variable-speed drives with the modular multilevel converter," in Proc. IEEE Energy Convers. Congr.Expo., 2013, pp. 1481–1488.

ISSN No: 2348-4845
International Journal & Magazine of Engineering, Technology, Management and Research
A Peer Reviewed Open Access International Journal

[16] S. Rohner, S.Bernet, M. Hiller, and R. Sommer, "Analysis and simulation of a 6 kV, 6 MVA modular multilevel converter," in Proc.IEEE 35th Annu. Ind. Electron. Conf., 2009, pp. 225–230.

[17] S. Rohner, S. Bernet, M. Hiller, and R. Sommer, "Modulation, losses, and semiconductor requirements of modular multilevel converters," IEEE Trans. Ind. Electron., vol. 57, no. 8, pp. 2633–2642, Aug. 2010.

[18] Q. Tu, Z. Xu, H. Huang, and J. Zhang, "Parameter design principle of the arm inductor in modular multilevel converter based HVDC," in Proc. Int. Conf. Power Syst. Technol., 2010, pp. 1–6.

[19] D. Schroder,¨ElektrischeAntriebe—Regelung von Antriebssystemen. New York, NY, USA: Springer-Verlag, 2009.

[20] S. Engel and R. De Doncker, "Control of the modular multi-level converter for minimized cell capacitance," in Proc. 14th Eur. Conf. Power Electron. Appl., 2011, pp. 1–10.

[21] P. Munch, D. Gorges, M. Izak, and S. Liu, "Integrated current control, energy control and energy balancing of Modular Multilevel Converters," in Proc. 36th Annu. Conf. IEEE Ind. Electron. Soc., 2010, pp. 150–155.

[22] K. Wang, Y. Li, Z. Zheng, and L. Xu, "Voltage fluctuation suppression method of floating capacitors in a new modular multilevel converter," in Proc. IEEE Energy Convers. Congr.Expo., 2011, pp. 2072–2078.

[23] M. Spichartz, V. Staudt, and A. Steimel, "Analysis of the module-voltage fluctuations of the modular multilevel converter at variable-speed drive applications," in Proc. 13th Int. Conf. Optim. Electr.Electron. Equipment, 2012, pp. 751–758.

[24] L. Harnefors, S. Norrga, A. Antonopoulos, and H.-P. Nee, "Dynamic modeling of modular multilevel converters," in Proc. 14th Eur. Conf. Power Electron. Appl., 2011, pp. 1–10.

Author Details

Mr.S.Jayaprakash received the Bachelor of Degree from the University of JNTUA, Anantapur, India, in 2012 and he is currently pursuing Post Graduate Degree in Annamacharya Institute of Technology & Sciences,Tirupathi. .

Mr.P.Munisekhar received Post Graduate degree from SITAMS,Chittoor He is currently working as a Assistant Professor, in Annamacharya Institute of Technology &Sciences,Tirupathi and he is currently pursuing Ph.D degree in JNTUA, Anantapur.